

Flame-retardant thermoplastics derived from plant cell wall polymers by single ionic liquid substitution

メタデータ	言語: eng 出版者: 公開日: 2019-11-15 キーワード (Ja): キーワード (En): 作成者: メールアドレス: 所属:
URL	https://doi.org/10.24517/00056097

This work is licensed under a Creative Commons Attribution-NonCommercial-ShareAlike 3.0 International License.



Electronic Supplementary Information

Fire-retardant thermoplastics derived from plant cell wall

by single ionic liquid substitution

Ryunosuke Nishita, Kosuke Kuroda, Shohei Ota, Takatsugu Endo, Shiori Suzuki,

Kazuaki Ninomiya, and Kenji Takahashi

Correspondence to: kkuroda@staff.kanazawa-u.ac.jp

Supporting Figures

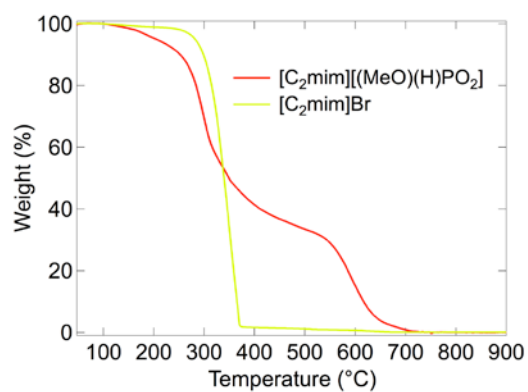


Fig. S1 TGA curves of $[\text{C}_2\text{mim}][(\text{MeO})(\text{H})\text{PO}_2]$ which were used in this study under air condition.

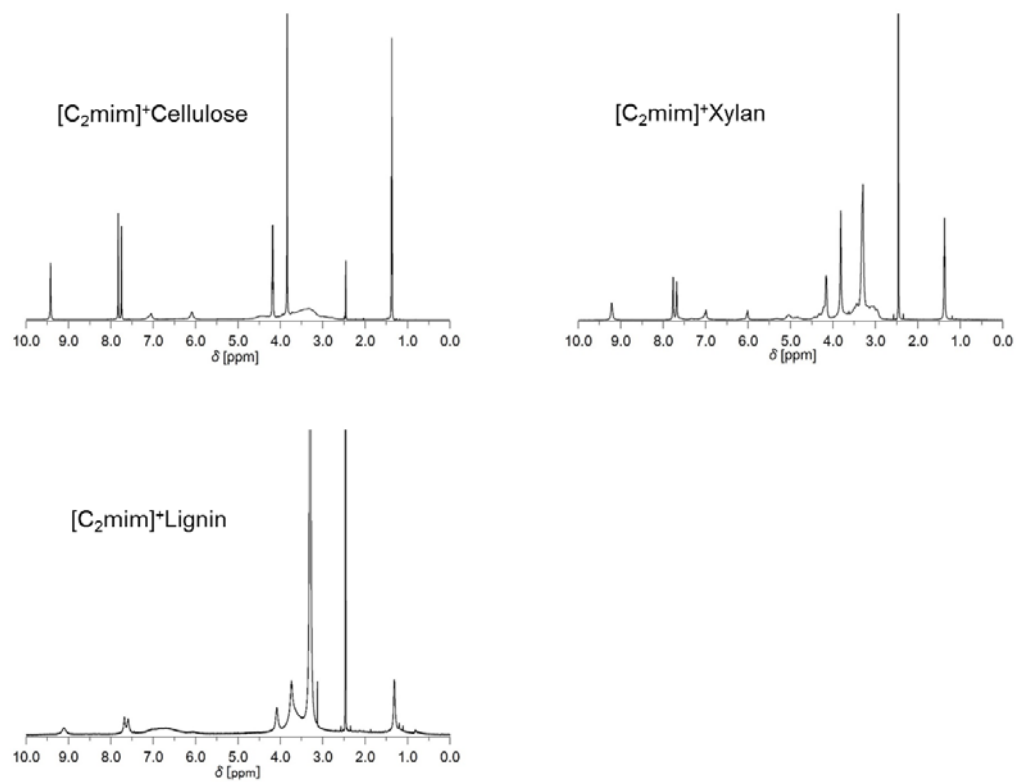


Fig. S2 ^1H NMR spectra of [C₂mim]⁺cellulose, [C₂mim]⁺xylan and [C₂mim]⁺lignin in DMSO-*d*₆.

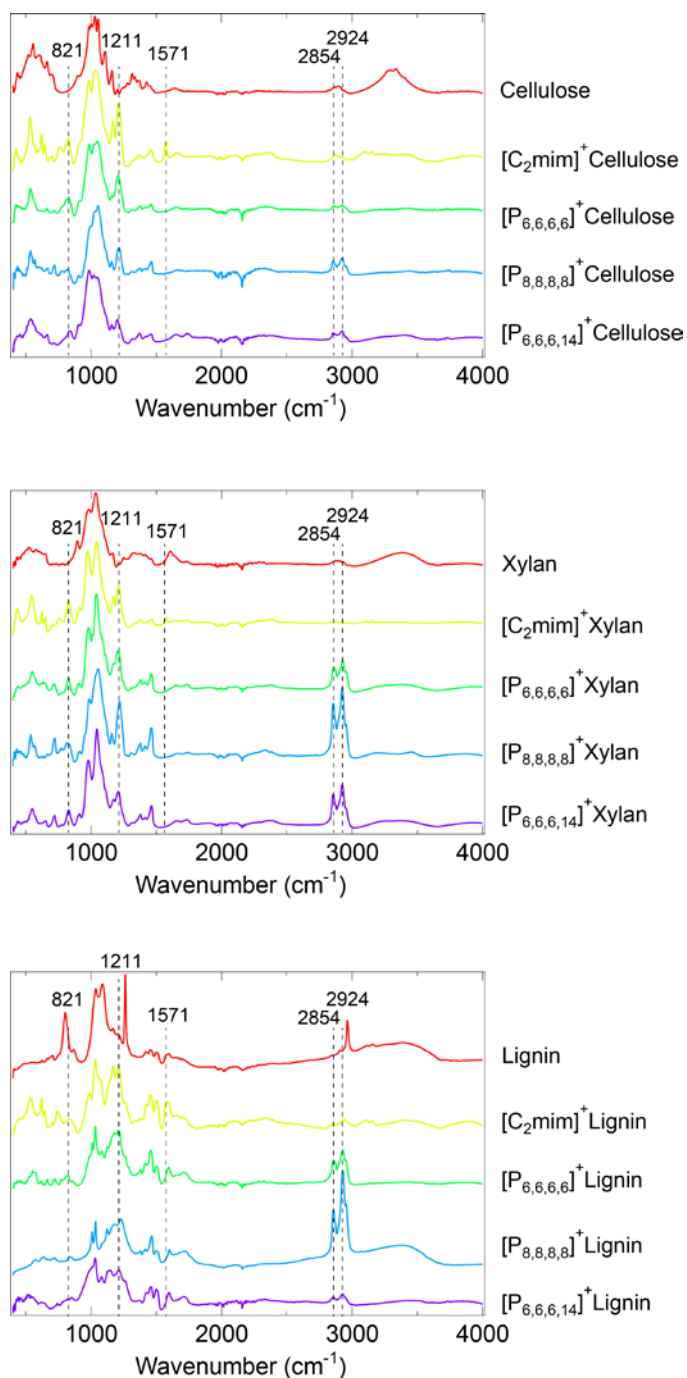


Fig. S3 FT-IR spectra of the underivatized and derivatized cellulose, xylan, and lignin.

The peaks derived from the P-O-C bond at 821 cm^{-1} , P=O bond at 1211 cm^{-1} , and C=N bond at 1571 cm^{-1} were detected in $[\text{C}_2\text{mim}]^+\text{cellulose}$, $[\text{C}_2\text{mim}]^+\text{xylan}$ and $[\text{C}_2\text{mim}]^+\text{lignin}$. The peaks derived from the C-H bond of phosphonium cation at 2854 and 2924 cm^{-1} were also detected in the spectrum of phosphonium-type derivatives. In the case of lignin derivatives, the signals are not strong due to the low derivatization ratio.

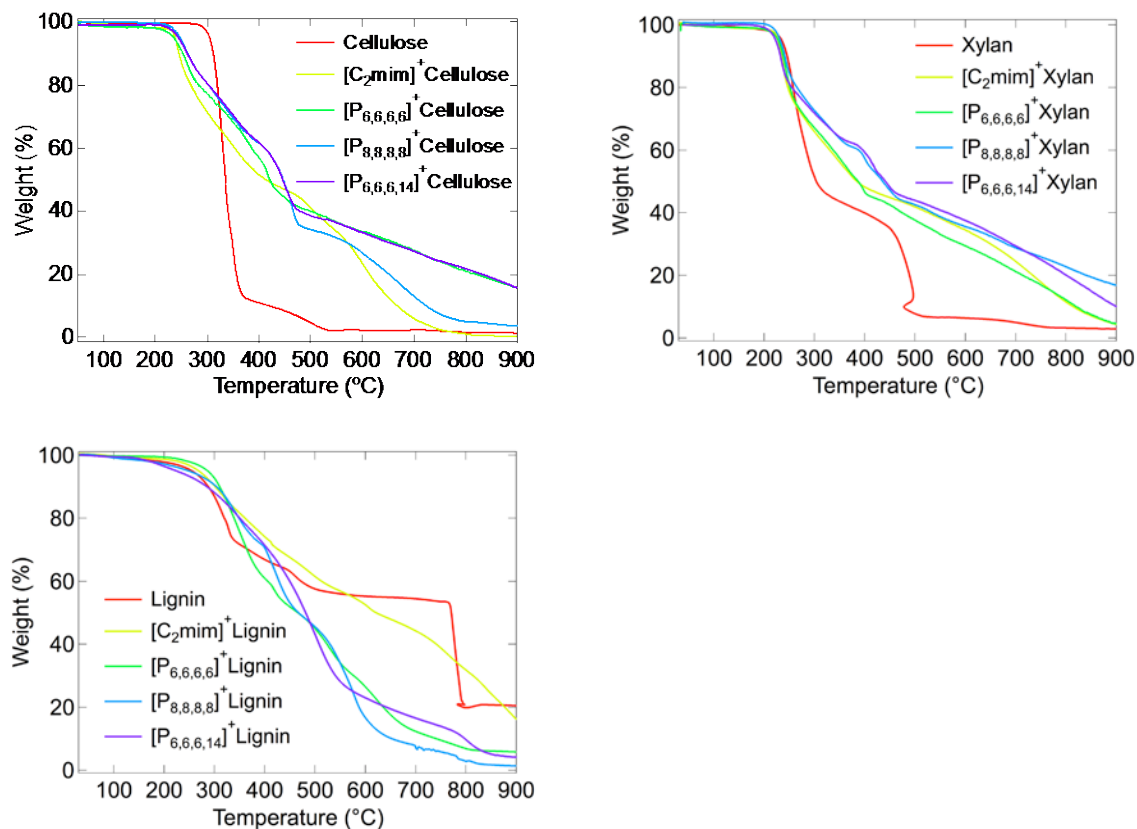


Fig. S4 TGA curves of the underivatised and derivitised cellulose, xylan, and lignin measured under air condition.

TG signals sometimes behaved abnormally (for example in the case of underivatised xylan) and the abnormal behaviour is attributed to the combustion of the samples because the samples were measured under air condition.

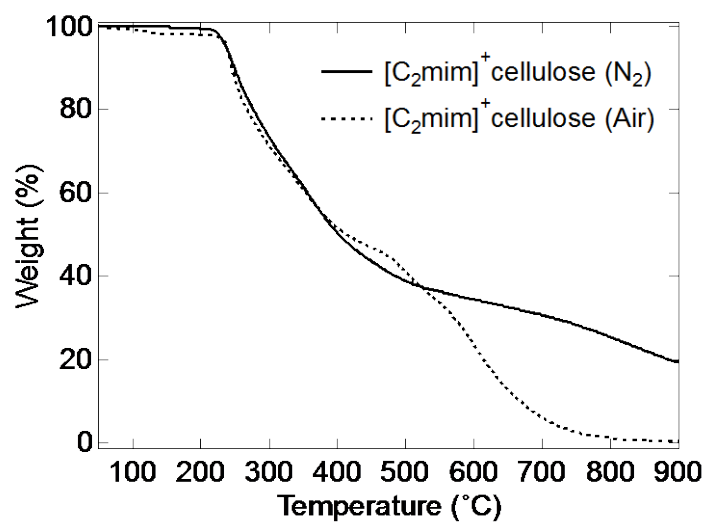


Fig. S5 TGA curves of [C₂mim]⁺cellulose measured under air and nitrogen gas conditions.

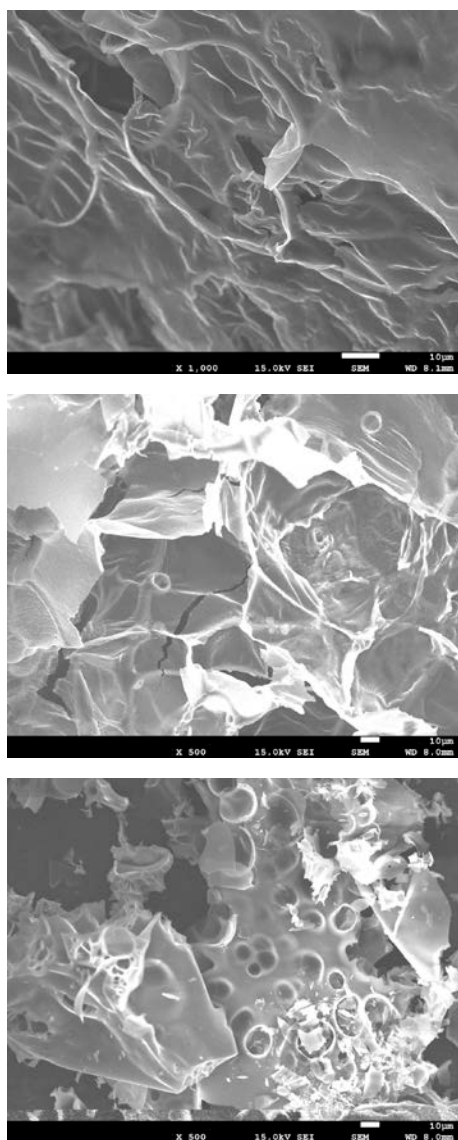


Fig. S6 SEM images of the char layers of $[\text{C}_2\text{mim}]^+\text{cellulose}$ (top), $[\text{C}_2\text{mim}]^+\text{xylan}$ (middle), $[\text{C}_2\text{mim}]^+\text{lignin}$ (bottom).

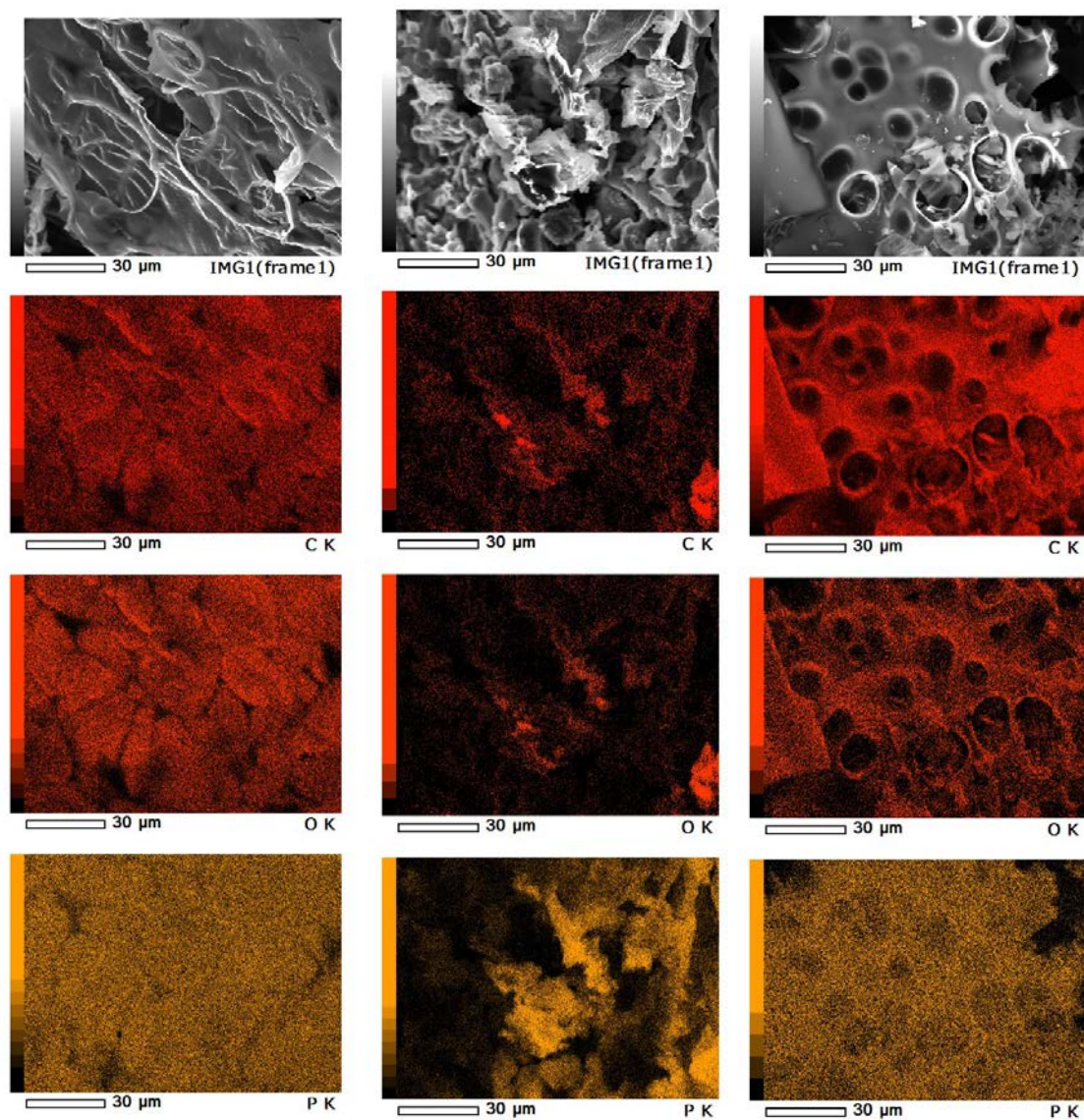


Fig. S7 SEM-EDX images of the char layers of [C₂mim]⁺cellulose (top), [C₂mim]⁺xylan (middle), [C₂mim]⁺lignin (bottom).

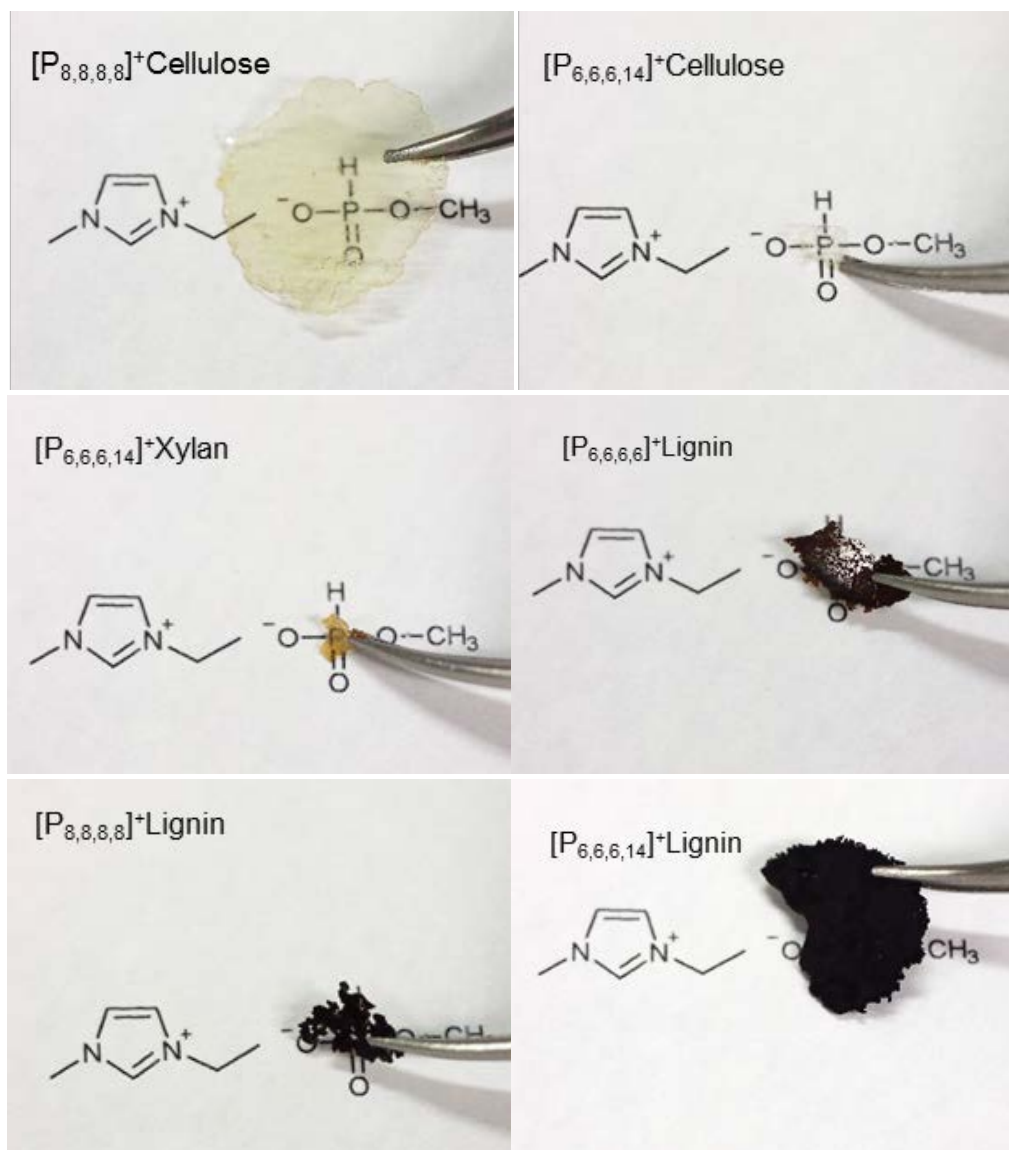


Fig. S8 Thin films of $[P_{8,8,8,8}]^+$ cellulose, $[P_{6,6,6,14}]^+$ cellulose, $[P_{6,6,6,14}]^+$ xylan, $[P_{6,6,6,6}]^+$ lignin, $[P_{8,8,8,8}]^+$ lignin, and $[P_{6,6,6,14}]^+$ lignin after hot pressing.

$[P_{8,8,8}]^+ \text{Cellulose}$



$[P_{6,6,6,14}]^+ \text{Cellulose}$



$[P_{6,6,6,14}]^+ \text{Xylan}$



$[P_{6,6,6,6}]^+ \text{Lignin}$



$[P_{8,8,8,8}]^+ \text{Lignin}$



$[P_{6,6,6,14}]^+ \text{Lignin}$



Fig. S9 Char formation of the thin films of $[P_{8,8,8}]^+ \text{cellulose}$, $[P_{6,6,6,14}]^+ \text{cellulose}$, $[P_{6,6,6,14}]^+ \text{xylan}$, $[P_{6,6,6,6}]^+ \text{lignin}$, $[P_{8,8,8,8}]^+ \text{lignin}$, and $[P_{6,6,6,14}]^+ \text{lignin}$ after burning and extinguish the fire.

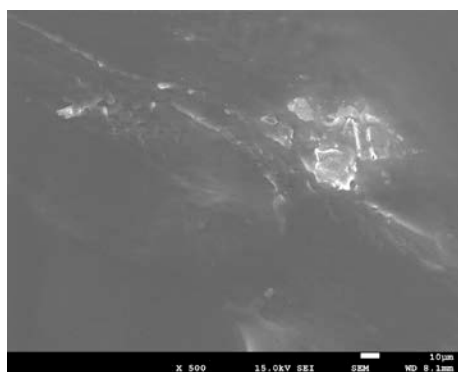


Fig. S10 A SEM image of the char layer of [P_{8,8,8}]⁺cellulose.

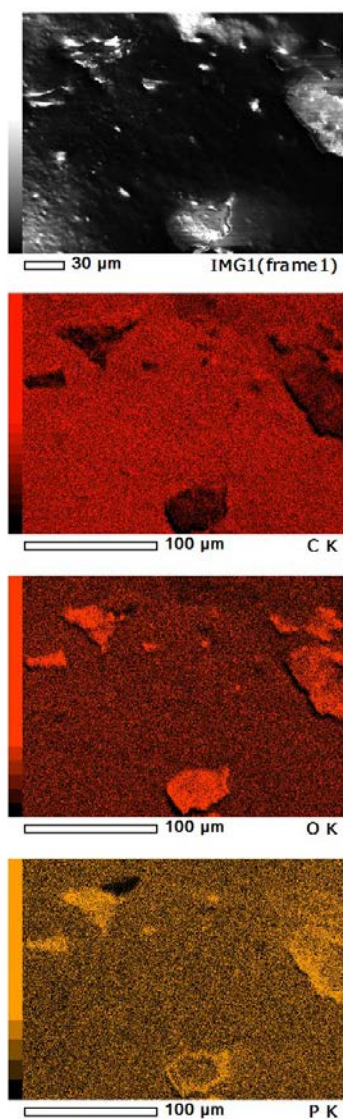


Fig. S11 A SEM-EDX image of the char layer of $[P_{8,8,8}]^+$ cellulose.

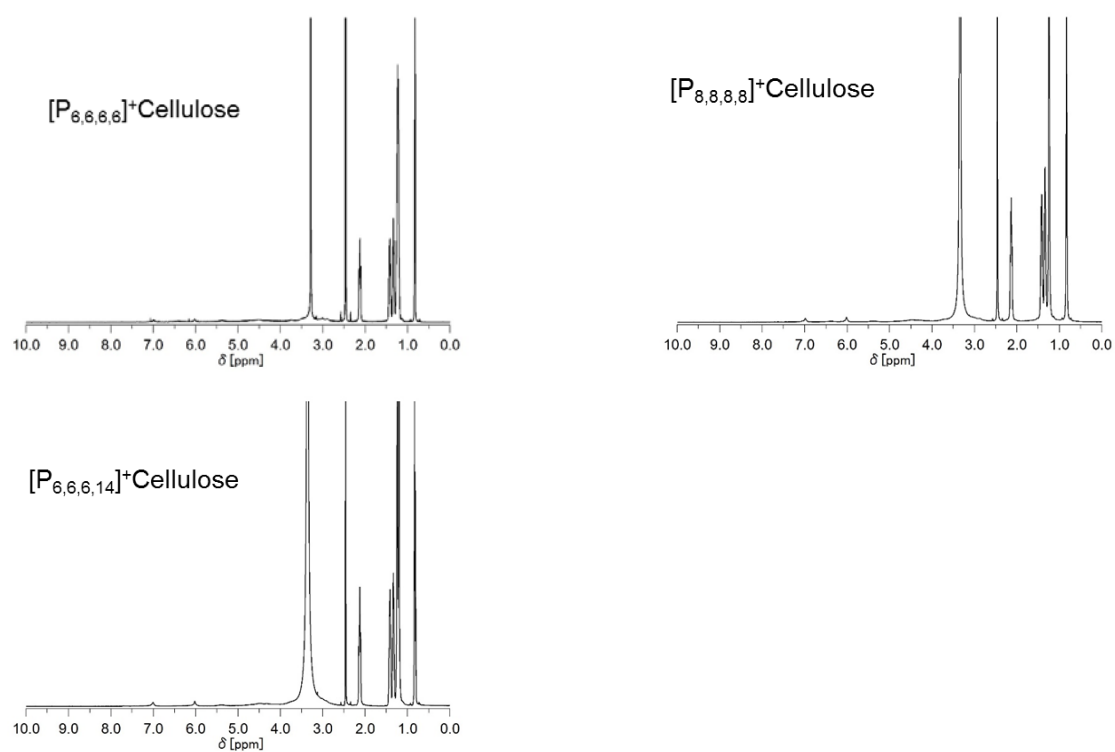


Fig. S12 ^1H NMR spectra of $[\text{P}_{6,6,6,6}]^+$, $[\text{P}_{8,8,8,8}]^+$, and $[\text{P}_{6,6,6,14}]^+$ cellulose in $\text{DMSO-}d_6$. The signal at 3.4 ppm is water.

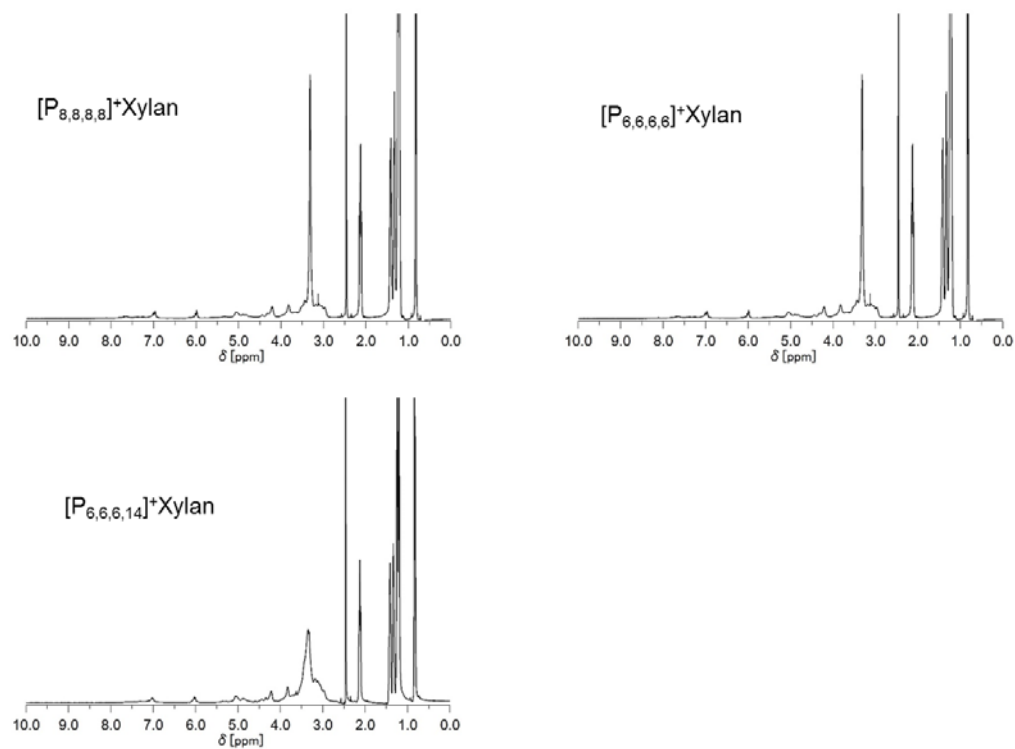


Fig. S13 ^1H NMR spectra of $[\text{P}_{6,6,6,6}]^+$, $[\text{P}_{8,8,8,8}]^+$, and $[\text{P}_{6,6,6,14}]^+$ xylan in $\text{DMSO-}d_6$. The signal at 3.4 ppm is water.

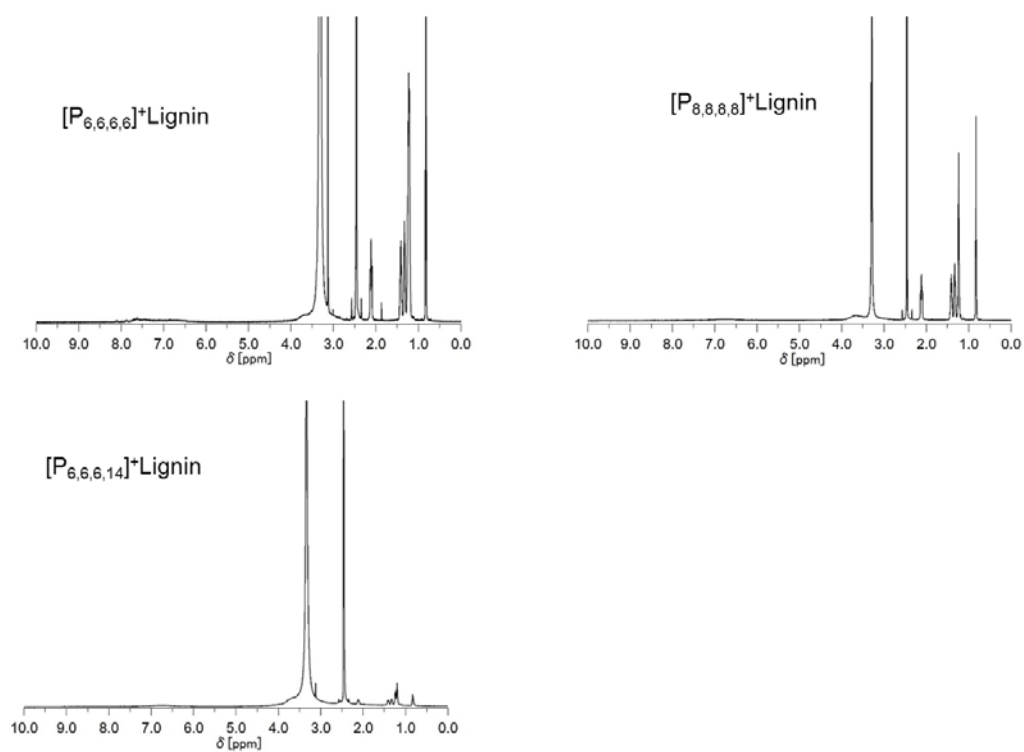


Fig. S14 ^1H NMR spectra of $[\text{P}_{6,6,6,6}]^+$, $[\text{P}_{8,8,8,8}]^+$, and $[\text{P}_{6,6,6,14}]^+$ lignin in $\text{DMSO-}d_6$. The signal at 3.4 ppm is water.